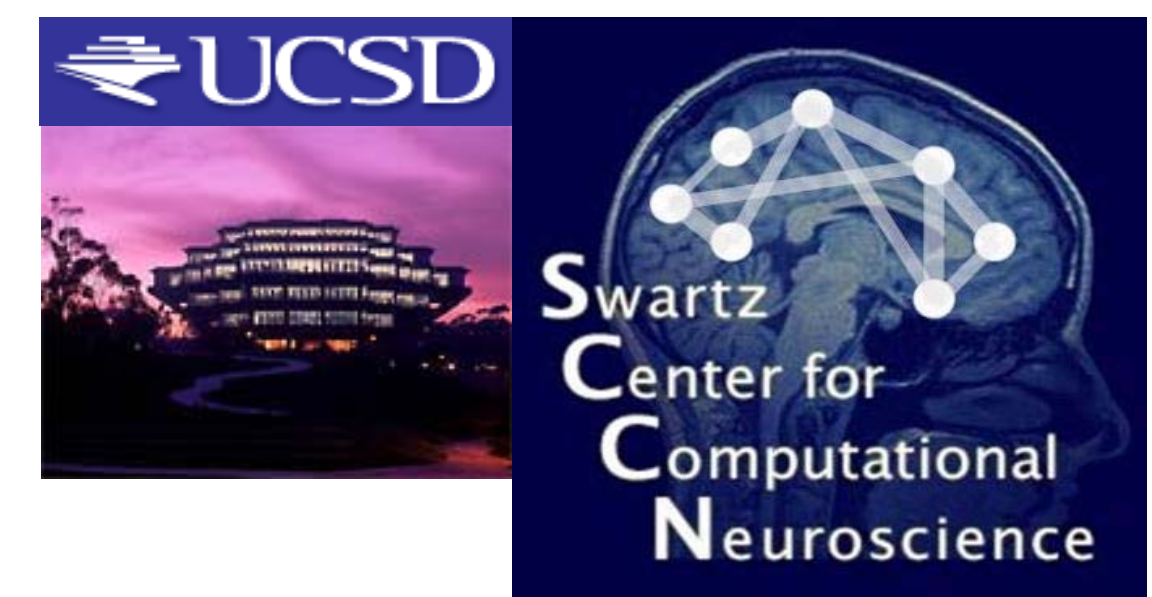


Emotion-related modulation of high-frequency EEG power



Julie Onton and Scott Makeig

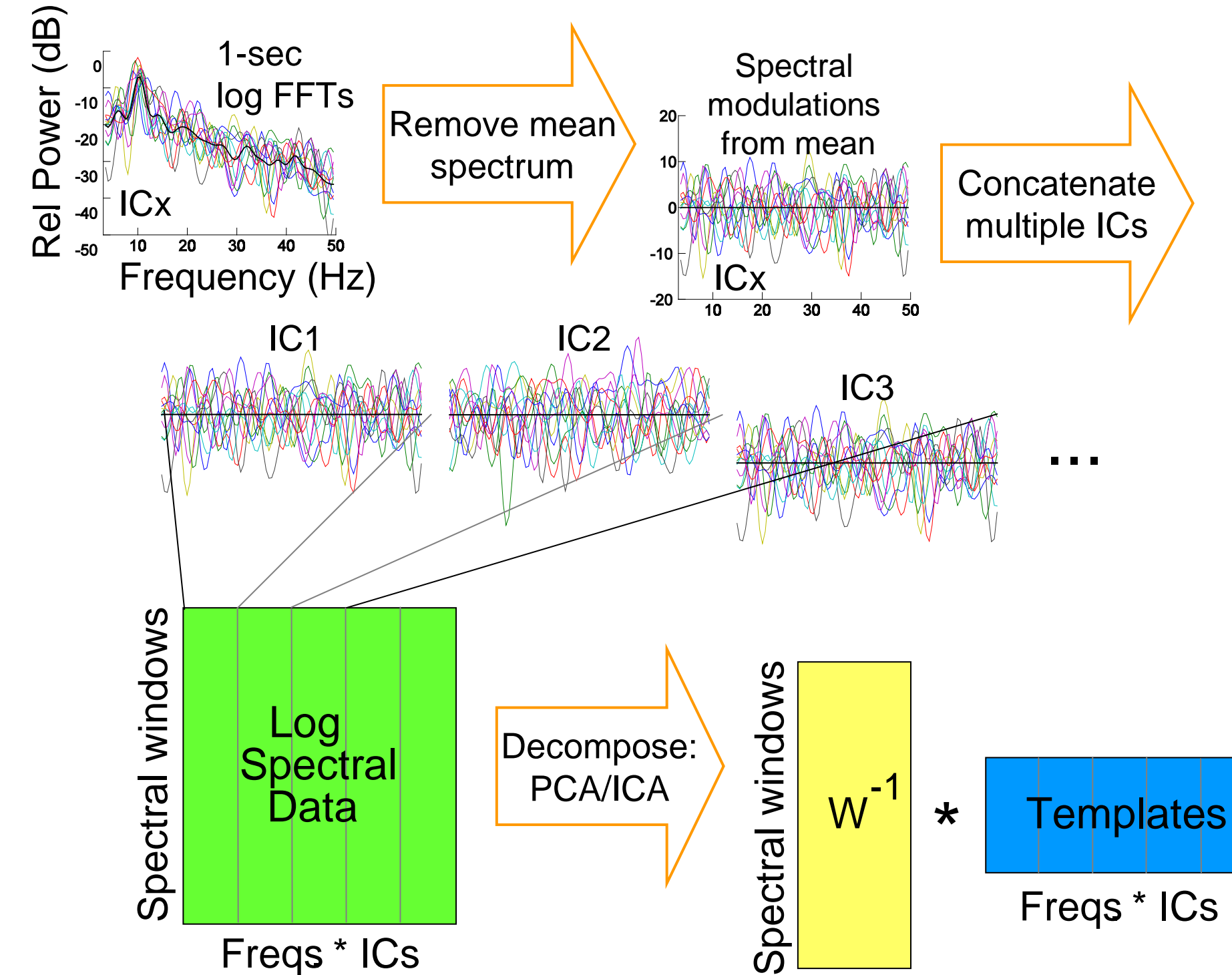
Institute for Neural Computation, UC San Diego, CA. <http://scn.ucsd.edu/>

BACKGROUND

It has long been assumed that high frequency brain activity cannot penetrate the dura, skull and scalp with sufficient strength to be detected, much less modeled, by available EEG analysis techniques. An additional difficulty is the presence of confounding EMG from scalp muscles which is always present in EEG scalp recordings. Here we introduce a new form of independent component analysis (ICA) applied to the log spectrogram of temporally independent component (IC) sources that separates the actions independent broadband, non-periodic modulations (IMs) of brain and muscle (EMG) source activities in high-density scalp EEG.

METHODS

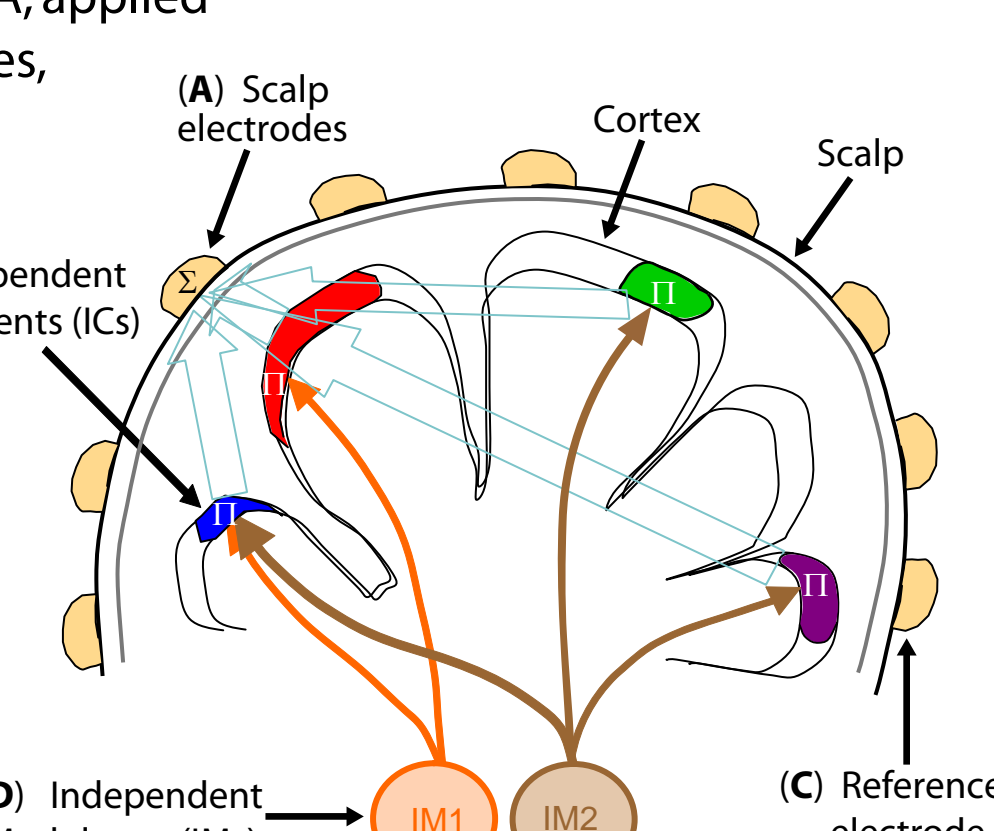
Subjects and Task. Young adults from the San Diego area (14 male, 18 female; age range: 18-38 (25.5 ± 5)) were guided through a series of emotional scenarios by a pre-recorded auditory narrative. Emotions were introduced with a short suggestion (~15-30 sec) of possible scenarios in which the emotion might arise and associated bodily sensations that might occur for the given emotion. Then during a self-paced silent period subjects attempted to imagine a suitable scenario, real or imaginary, and to experience the suggested emotion. Subjects were asked to maintain each emotional state for ~3-5 min. Data presented here were extracted from these emotional imagination periods. EEG data were submitted to extended infomax ICA (Lee et al., 1999) using the *binica* (Makeig et al., 1997) in the EEGLAB toolbox (Delorme, 2004).



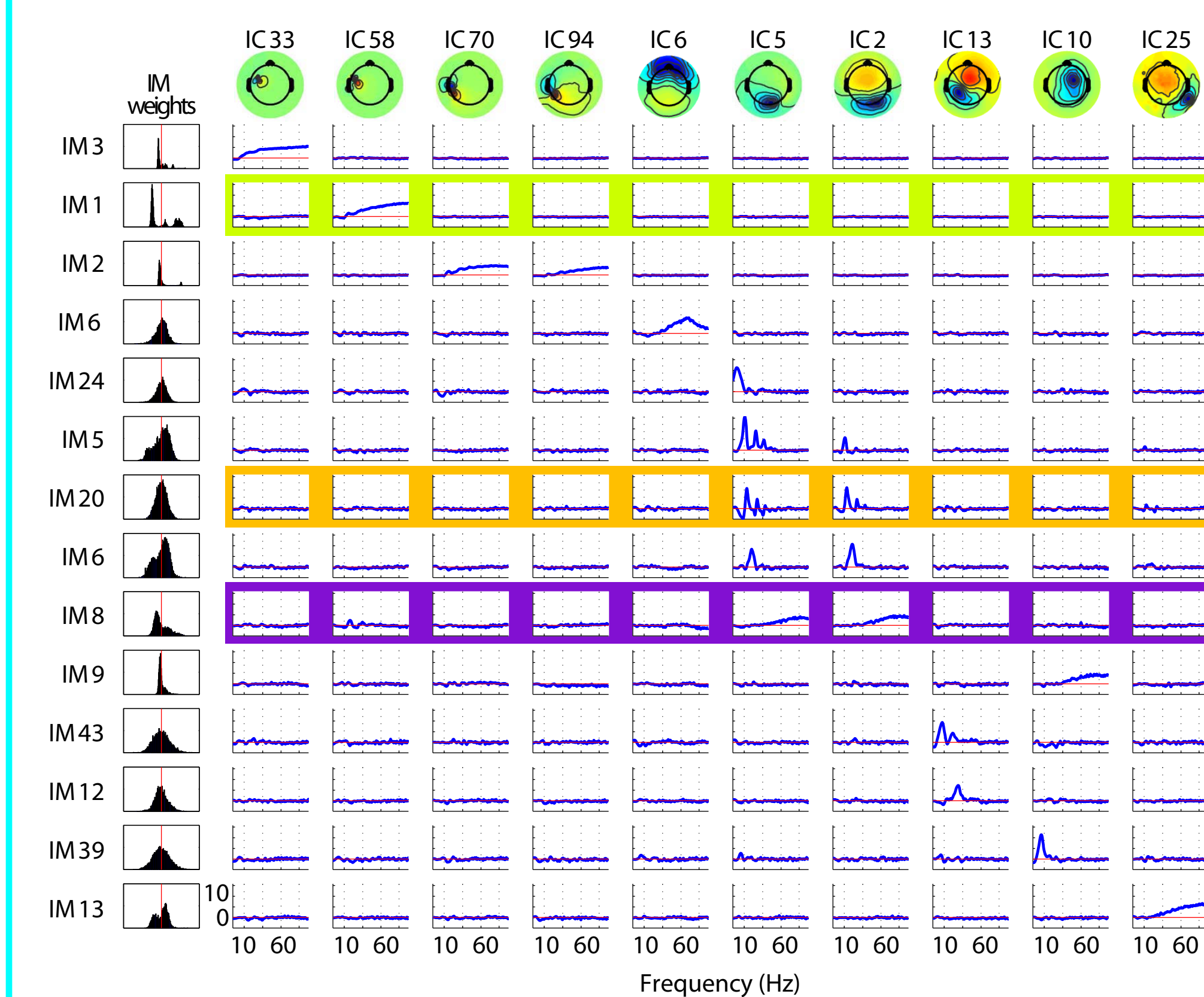
Modulator Decomposition. For each subject, data were extracted from event-free periods during which the subjects reported experiencing the requested emotion. These data were divided into 50%-overlapping 1-sec windows and then concatenated across emotions. For each selected independent component (IC) process, a fast Fourier transform (FFT, Welch method) was performed on each 1-sec window between 1 Hz and 128 Hz. The result of this decomposition was transformed into log power ($dB = 10 \cdot \log_{10}(\text{power})$). For each component, the mean log power spectrum was subtracted from each epoch so that only fluctuations from the mean spectrum remained (see diagram). Power fluctuations for 10-40 selected components were then concatenated to yield a matrix with size (windows x frequencies * ICs). The resulting matrix was submitted to ICA after removing all but the first 100 principal dimensions of the data by principal component analysis (PCA). ICA returned maximally independent modulation (IM) modes or templates, as well as the weight of each IM in each time window (see diagram). To find common IMs across subjects, IM templates from each IC were represented independently and submitted to cluster analysis, sorting first for the frequency range with the highest absolute value and then further clustered by linking templates with minimal correlation distance. ICs of an IM were labeled as 'co-modulated' when more than one template from a single IM were independently grouped into the same cluster.

INDEPENDENT MODULATORS (IMs)

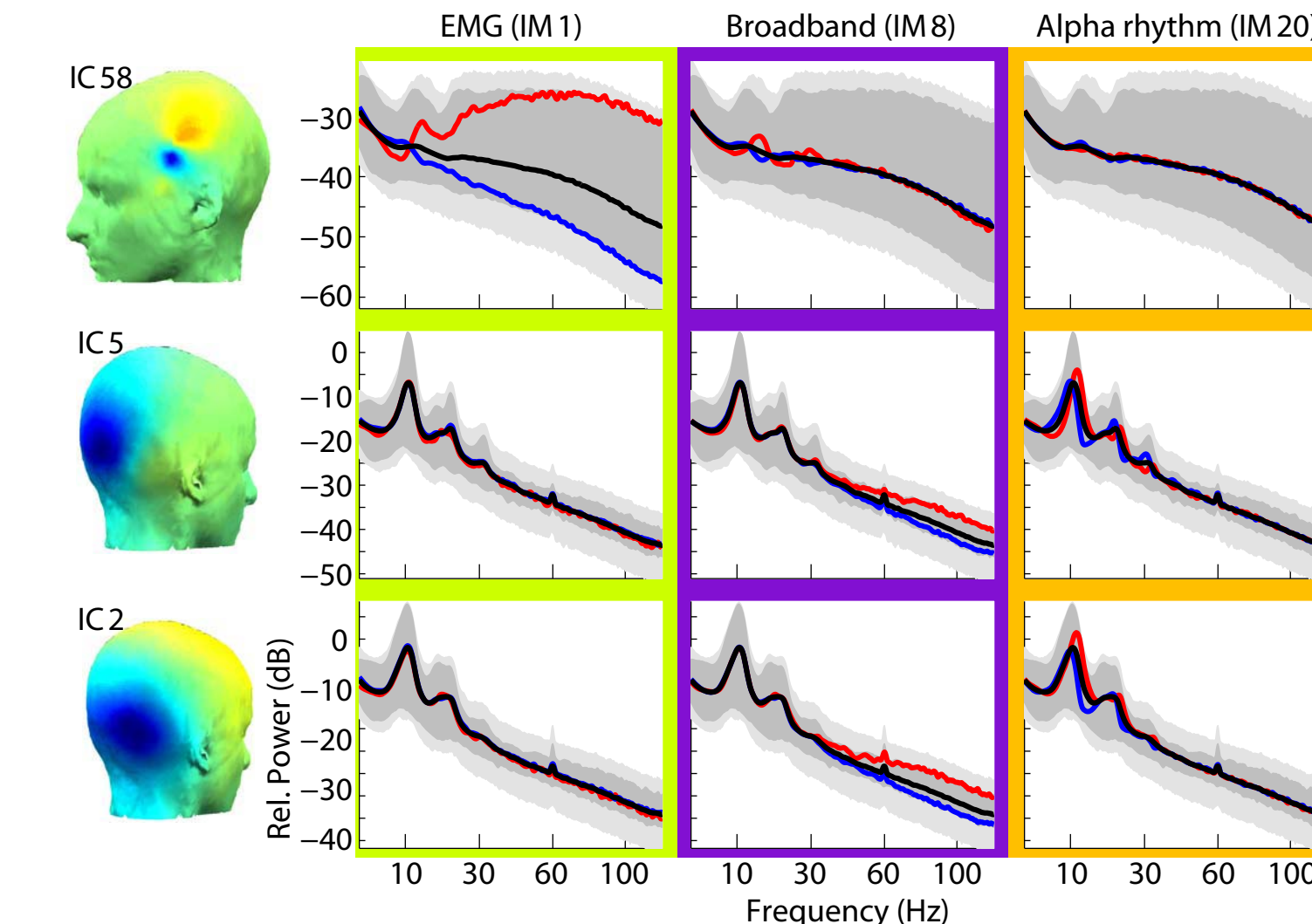
Independent spectral modulators of scalp EEG signals. ICA, applied to EEG data recorded at a large number of scalp electrodes, identifies (A) temporally distinct (independent) signals generated by partial synchronization of local field potentials within cortical patches (B), the resulting far-field potentials summed (Σ), in differing linear combinations, at each electrode depending on the distance and orientation of each cortical patch generator relative to the (A) recording and (C) reference electrodes. On average, power in the cortical IC signals decrease monotonically with frequency, but also exhibit continual, marked, and complex variations across time. Rather than viewing these variations as occurring independently at each frequency, spectral modulations may be modeled as exponentially weighted influences of several distinct but possibly overlapping modulator (IM) processes (D) that independently modulate via multiplicatively scaling the activity spectra of one or more independent component (IC) signals. On converting the IC spectra to log power, combined IM influences on IC spectra are converted to log-linear weighted sums of IM influences, allowing a linear ICA decomposition of the IC log power spectra to separate the effects of the individual IM processes (D) on power at selected frequencies of IC sources (B).



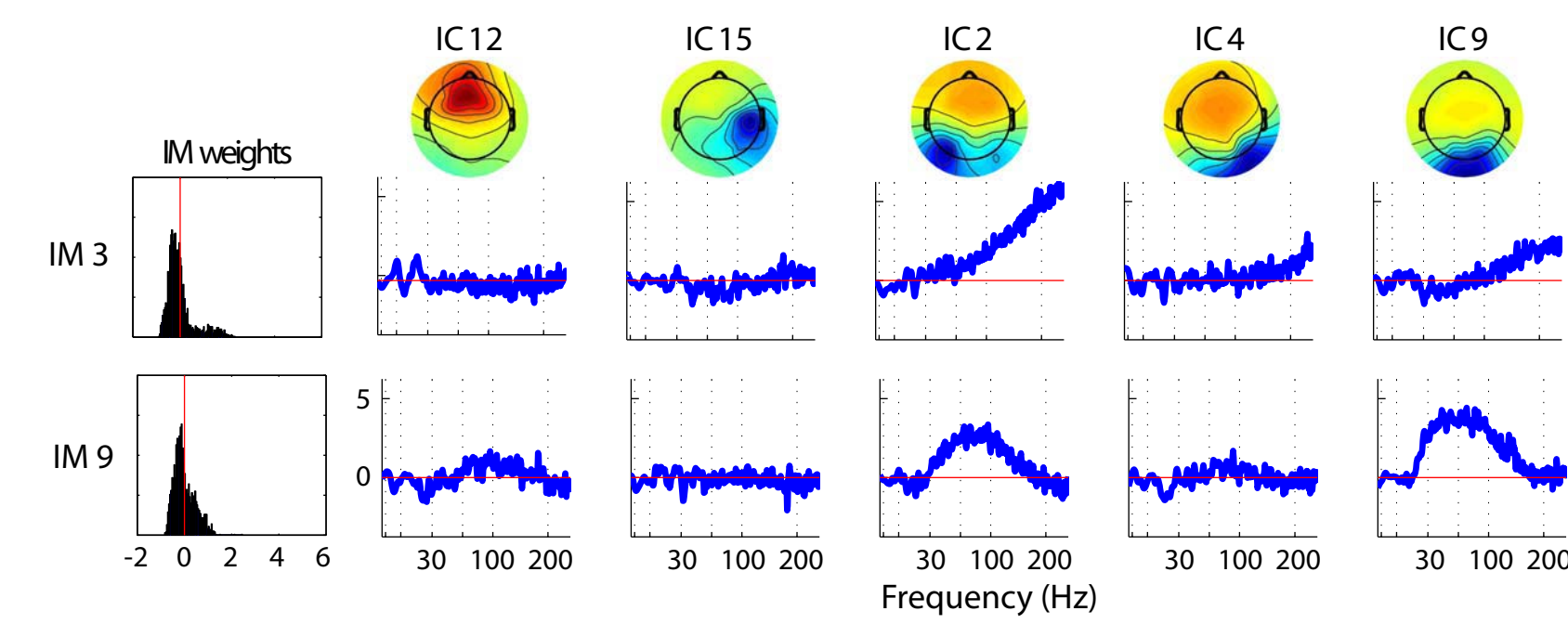
EXAMPLE IM DECOMPOSITION



Single-subject decomposition of log-spectral power modulations across an hour-long experimental session. The fourteen IMs visualized here (14 rows) represent major classes of spectral modulation of 10 of the 16 ICs (rightmost 10 columns) entered into the log spectral decomposition for this subject. The leftmost column shows histograms of the time-window weights for each IM. The top four IMs (IMs 1-3, 6) are examples of broadband modulators affecting activity in scalp muscle ICs (IMs 1-3) and a putative ocular motor IC (IM6); note the muscle IMs' multimodal weight histograms. The other IMs (below) affect only brain ICs, either with a broadband pattern (IMs 8, 9, 13) else in the theta (IM24), alpha (IMs 5, 20, 39, 43), or beta (IMs 6, 12) frequency ranges.

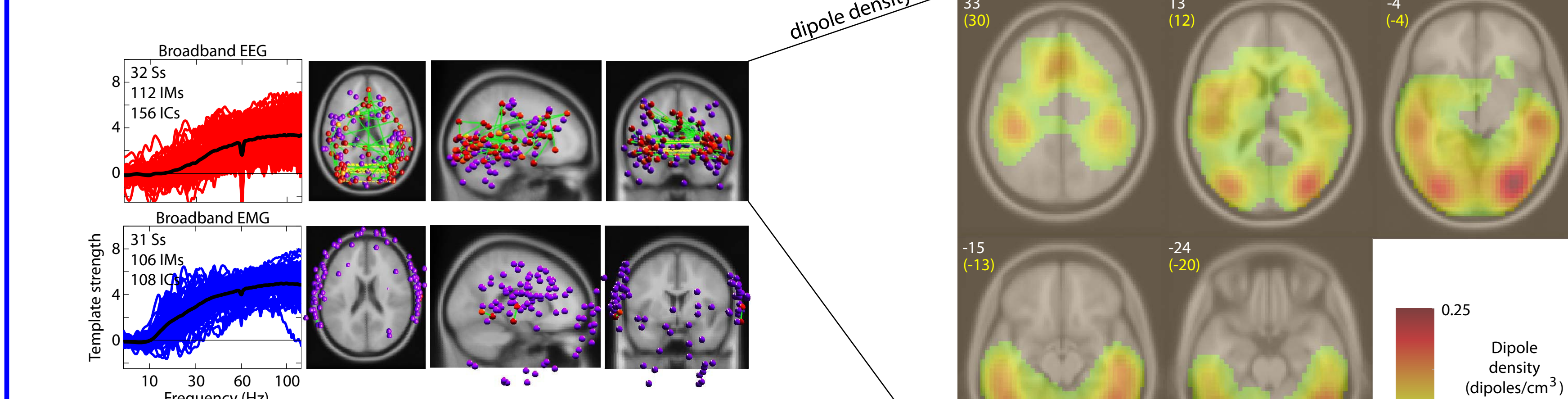


Effects of brain and muscle modulators on independent component spectra. Maximal effects of three IMs (columns) on the power spectra of three ICs (rows) are shown via their maximal (red traces), minimal (blue traces), and mean (black traces) log power spectra. Dark grey areas represent the 1st and 99th percentiles of the PCA-reduced spectral data.



Broadband modulators of a data set with higher sampling rate. A sampling rate of 512 Hz in this dataset allowed an upper frequency limit of 256 Hz, revealing variable broadband patterns between 128 Hz and 256 Hz.

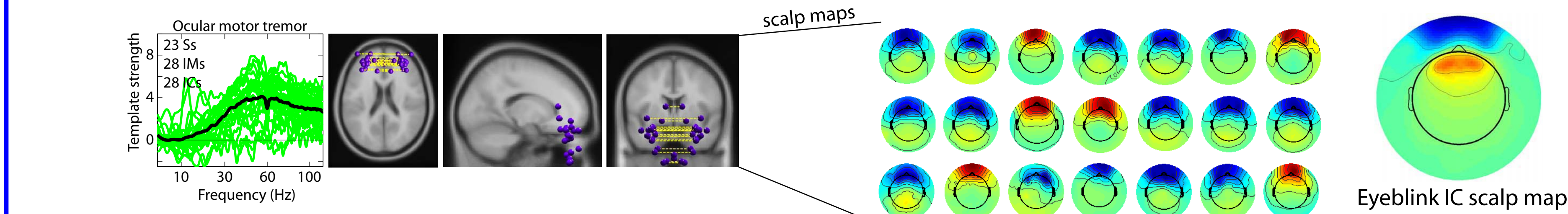
GAMMA IMs ACROSS SUBJECTS



Broadband modulators of brain and scalp muscle components. Brain and scalp muscle ICs are separately modulated by IMs with similar broadband high-frequency templates (upper rows). The left column shows broadband templates for each IC category (black trace is the mean). The right three columns show equivalent dipole locations of the affected ICs. Dipole locations for scalp muscle ICs are outside the brain volume (middle row). Green lines in dipole plots connect ICs co-modulated by the same IM and the colors of the dipole spheres (yellow to red) indicate the relative strength of modulation (yellow = 50%, to red = 100% of maximal). Purple spheres indicate individually modulated ICs.

Equivalent dipole density of ICs affected by broadband IMs. Spatial density profile of equivalent dipoles (in total dipoles per cubic cm among 154 broadband IMs from 32 subjects), obtained by convolving each dipole location with a 3-D Gaussian blur (1-cm std. dev.) and then summing (after normalizing for boundary effects). White integers above and to the left of each slice image give their standard MNI brain z-axis coordinates, yellow text the nearest Talairach z-axis coordinates. Values below 0.04 dipoles/cm³ are set to 0.

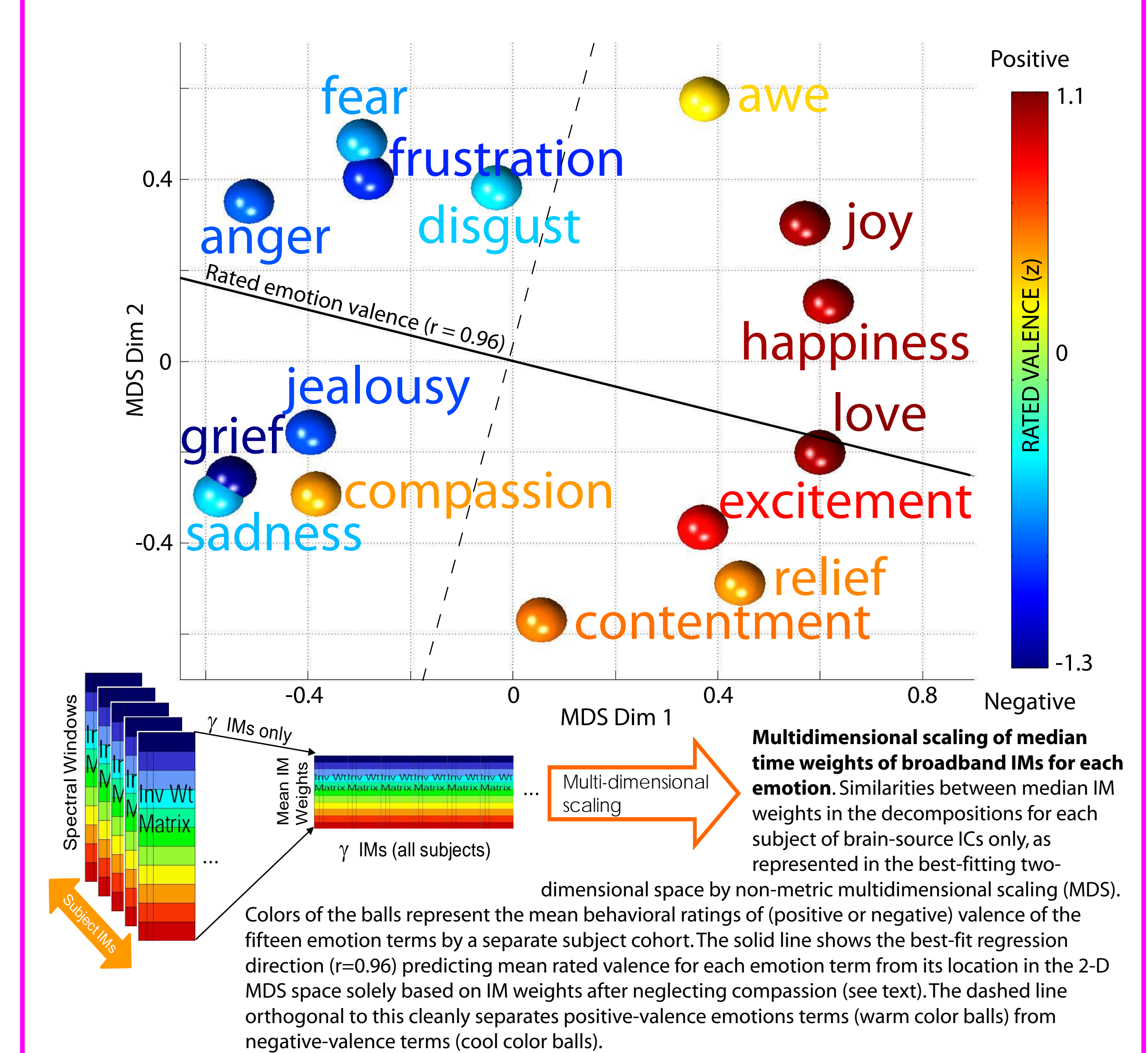
OCULAR MOTOR TREMOR



A distinct cluster of putative ocular motor IMs have a peak effect near 50 Hz on ICs many of whose bilaterally symmetric equivalent dipole models (bottom right panels) are located near the eyes. (ICs whose best-fit equivalent dipole model comprised two bilaterally symmetrical dipoles are represented with a dotted yellow line connecting the dipole pair).

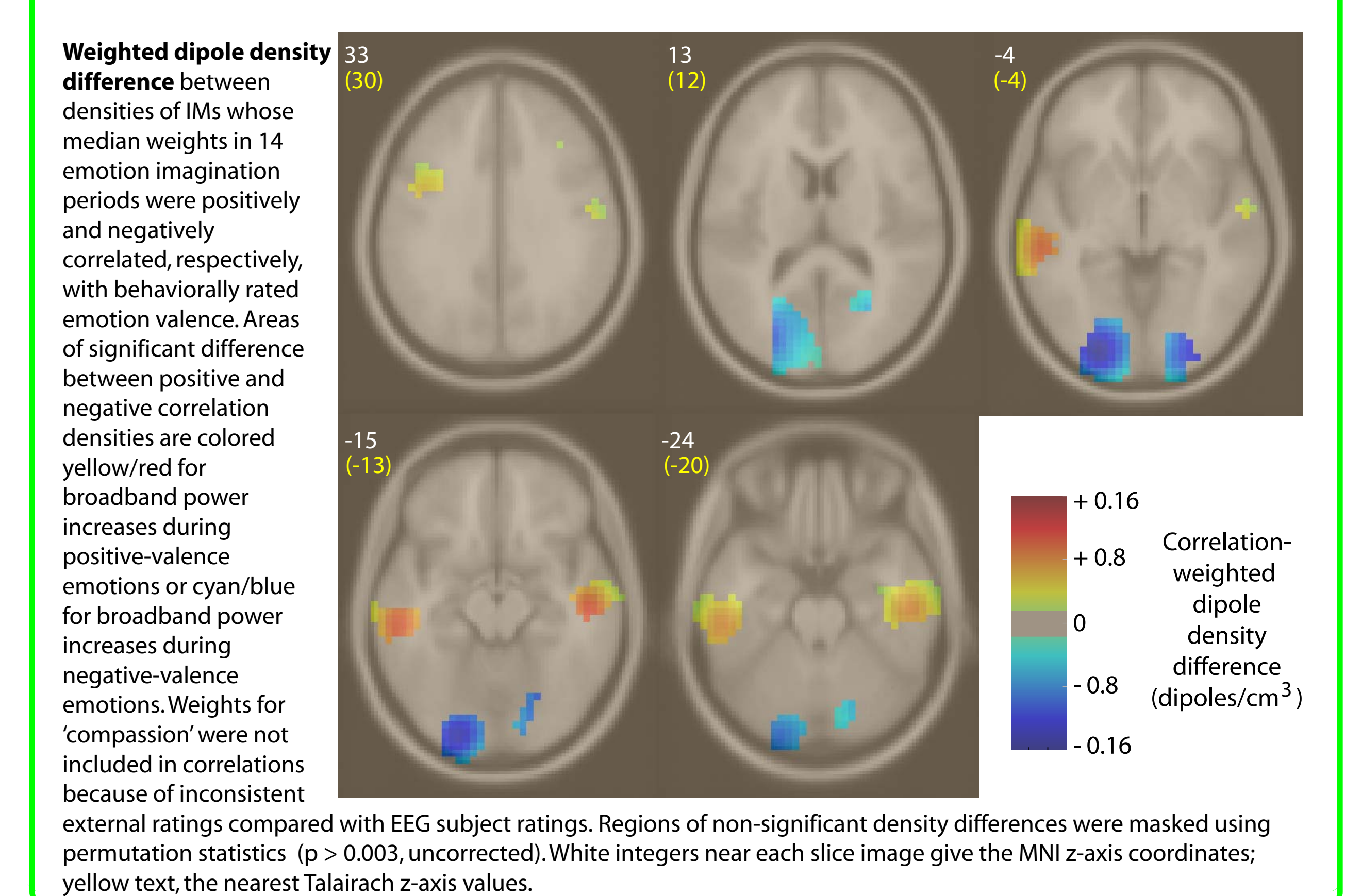
Scalp maps from the ICA inverse weight matrix for each of the inferior frontal ICs reveal a characteristic pattern that is distinguishable from eye blink by the lack of polarity reversal (compare eyeblink IC map at right).

EMOTION SPACE



Multidimensional scaling of median time weights of broadband IMs for each emotion. Similarities between median IM weights in the decompositions for each subject of brain-source ICs only, as represented in the best-fitting two-dimensional space by non-metric multidimensional scaling (MDS). Colors of the balls represent the mean behavioral ratings of (positive or negative) valence of the fifteen emotion terms by a separate subject cohort. The solid line shows the best-fit regression direction ($r=0.96$) predicting mean rated valence for each emotion term from its location in the 2-D MDS space solely based on IM weights after neglecting compassion (see text). The dashed line orthogonal to this cleanly separates positive-valence emotion terms (warm color balls) from negative-valence terms (cool color balls).

GAMMA AND VALENCE CORRELATION



Weighted dipole density difference between densities of IMs whose median weights in 14 emotion imagination periods were positively and negatively correlated, respectively, with behaviorally rated emotion valence. Areas of significant difference between positive and negative correlation densities are colored yellow/red for broadband power increases during positive-valence emotions or cyan/blue for broadband power increases during negative-valence emotions. Weights for 'compassion' were not included in correlations because of inconsistent external ratings compared with EEG subject ratings. Regions of non-significant density differences were masked using permutation statistics ($p > 0.003$, uncorrected). White integers near each slice image give the MNI z-axis coordinates; yellow text, the nearest Talairach z-axis values.

SUMMARY

- ✓ High frequency gamma activity can be detected in scalp-level EEG recordings and is separable from muscle gamma
- ✓ Spectral decomposition reveals high frequency power as broadband modulations between ~15 and 250 Hz
- ✓ Broadband power modulations tend to vary with emotional valence, but in complex ways